Failure study on laser welds of dual phase steel in formability testing

M. S. Xia[1,2], M. L. Kuntz[1], Z. L. Tian[2] and Y. Zhou*[1]

In this paper, the formability of YAG and diode laser welded blanks of a dual phase (DP) steel with banded martensite was investigated by using limiting dome height (LDH) testing method. One high strength low alloy (HSLA) steel with equiaxed ferrite matrix was included for comparison. Both steels had a ferrite matrix and dispersed secondary phase, namely martensite and carbide. The failure mode and dome height at fracture were examined on both parent metals and welded blanks. It was found that the failure pattern of DP parent metal was determined by its rolling direction. With increasing plastic strain, voids initiated along interfaces between ferrite/martensite due to decohesion between two phases and propagated preferentially along the interface. For DP welded blanks, dome test failures occurred within the softened zone in the heat affected zone (HAZ) regardless of the orientation between weld and rolling direction. Voids formed at the interfaces between ferrite and tempered martensite. The presence of the softened HAZ zone led to dramatic LDH decrease compared to the parent metal. The diode laser welded blanks had a lower dome height than that of YAG laser welded blanks due to their more severe HAZ softening. In comparison, HSLA parent metal and welded blanks exhibited almost the same LDH values and showed insensitivity to welding process. The failure of HSLA welded blanks initiated from the weld and propagated perpendicular to the unaffected base metal.

Keywords: Formability, Dual phase steel, Laser welding, HAZ softening, Rolling direction, Fracture modes

Introduction

New grades of advanced high strength steel (AHSS) have recently been used to improve autobody crash performance without a weight penalty. Among them, dual phase (DP) steels have seen increasingly used in critical components where high strength and continuous yielding help to increase energy absorption during a crash. There is significant interest in increasing the application of AHSS to other components and assemblies, such as in tailored blanks for formed panels. This will help to achieve environmental goals, improved vehicle response, and increased occupant safety through vehicle light weighting by compounded reduction in body weight.

The term 'dual phase' refers to a particular class of steels with two phase ferrous microstructure, namely the relatively soft body centred cubic ferrite and the relatively hard body centred tetragonal martensite, together with the distinctive processing route for their production. The beneficial ferrite martensite mixture in DP steels is typically produced after annealing in the so called intercritical temperature range, where ferrite and austenite are stabilised. This annealing is immediately followed by rapid cooling (or quenching) to transform the austenite into martensite.[1] Compared to high strength low alloy (HSLA) steels, DP steels possess slightly lower yield strength (YS). However, a continuous flow behaviour results in high and uniform total elongation, with high initial strain hardening and significantly higher tensile strengths.[2] It is these good mechanical characteristics of DP steels that have made them appealing to the automotive industry.

While DP steels typically exhibit good formability due to their unique microstructural makeup, changes in local material properties caused by welding tend to negatively affect the formability of tailor welded blanks (TWBs).[3] For example, heat affected zone (HAZ) softening frequently occurs as a result of martensite tempering, especially for DP steels with high martensite content. The softened zone is characterised by lower hardness and strength than the parent metal. Concurrently, in the fusion zone, hardening readily occurs, especially with low heat input welding processes.[4] Generally, these effects result in deterioration of the overall mechanical performance of weldments.[3] The application of DP steels has thereby been hindered due to challenges in welding and forming operations.[5–7]

In previous research on failure of TWBs in biaxial stretch forming, two distinct failure modes have been observed. If the thickness and strength ratios of the two sheets are such that weld line movement is limited during

[1]Centre for Advanced Materials Joining, University of Waterloo, Waterloo, ON, Canada
[2]Central Iron and Steel Research Institute, Beijing, China

*Corresponding author, email nzhou@mecheng1.uwaterloo.ca

Published by Maney on behalf of the Institute
Received 12 December 2007; accepted 30 January 2008
DOI 10.1179/174329308X299977

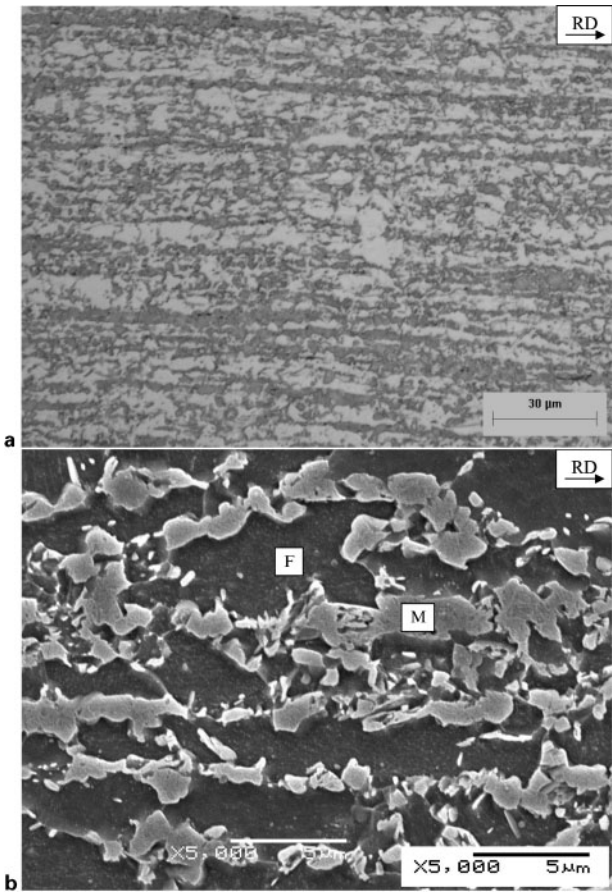

a optical; *b* SEM

1 Base metal microstructure of DP980

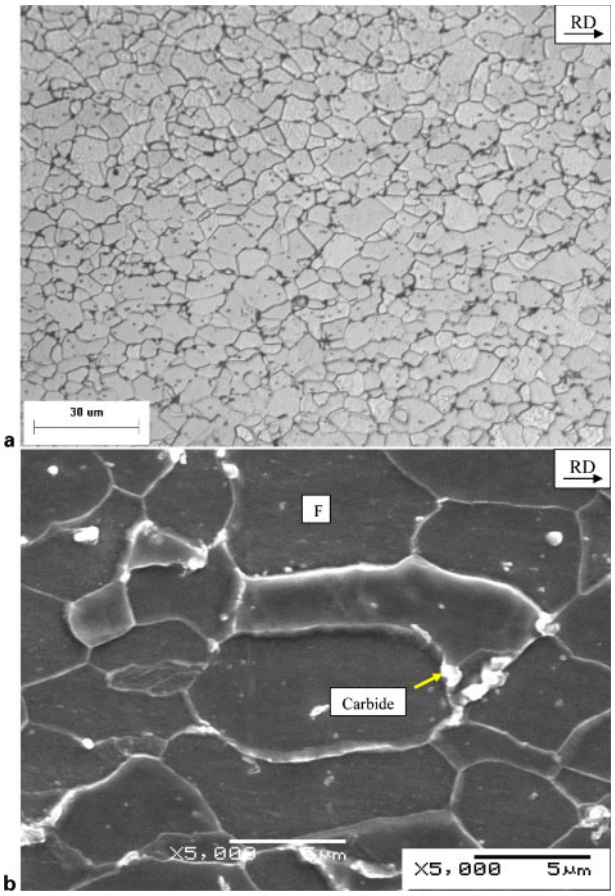

a optical; *b* SEM

2 Base metal microstructure of HSLA

forming, failure tends to initiate in the hardened weld metal and propagate perpendicularly into the base metal.[8] On the other hand, if there is significant weld line movement due to strength or thickness mismatch, the failure tends to occur parallel to the weld in the weaker of the two base metals when the ultimate tensile stress is exceeded.[8] However, a third failure mode, namely failure at the HAZ, has been recently observed in TWBs of high strength DP steels due to the softened zone formation.[3] Furthermore, failure in the softened HAZ occurred irrespective of the orientation of the weld to the rolling direction.

As a result, it is clear that HAZ softening can deteriorate the formability of AHSS welded blanks. However, details of failure initiation and propagation on a microscale level during biaxial testing are still unknown. Therefore, one objective of this study is to characterise the failure mode of DP parent metal and its welded blanks on a microscale level. The softened zone mechanical properties have also been evaluated with a thermal simulation technique to further clarify its formability behaviour.

Experimental procedures

Materials

Two sheet steels were investigated, including a 980 MPa dual phase (DP980) and a 450 MPa HSLA (HSLA450). Both of the steels were zinc coated: the DP980 was galvannealed and the HSLA450 was hot dip galvanised. The thicknesses of the DP980 and HSLA sheet were 1·2 and 1·14 mm respectively. The steels' chemistries are summarised in Table 1. Both steels were composed of ferrite as matrix and dispersed secondary phase, namely martensite and carbide. The martensite volume fraction of the DP980 steel, as determined through area analysis, was about 50 pct. Inspection of the microstructure under optical microscopy in Fig. 1*a* showed the typical DP structure consisting of martensite islands within the polygonal ferrite matrix; however, the distribution of martensite was severely banded resulting in martensite 'stringers'. Scanning electron microscopy observation in Fig. 1*b* showed that ferrite was the continuous phase. Examination of the HSLA microstructure under optical microscopy, shown in Fig. 2*a*, revealed an equiaxed ferrite matrix. A dispersion of carbides at the grain boundaries and within the ferrite grains, as shown in Fig. 2*b*, was observed under SEM.

Laser properties

The diode laser used was a Nuvonyx ISL-4000L mounted on the manipulator arm of a Panasonic VR-16 welding robot. This laser head comprises four water cooled heat sinks each containing 20 individual laser diodes, with condensing optics to deliver a combined

Table 1 Chemical compositions of investigated steel, wt-%

Steel	C	Mn	Mo	Si	Cr	Al	B
DP980	0·135	2·1	0·35	0·05	0·15	0·45	0·007
HSLA	0·056	0·64	0·015	0·026	0·09	0·06	0·00017

rectangular beam of $12 \times 0{\cdot}5$ mm. The Haas HL3006D Nd:YAG laser employs fibre beam delivery from a remote laser system to the final delivery optics. This laser output had a gantry mounted optical system, and magnetic clamping mechanism to hold the workpiece. Full power of each laser was used for welding: 4 and 3 kW respectively. The detailed characteristics of these lasers are shown in Table 2.

Laser welding can be carried out in two different modes, i.e. keyhole or conduction mode welding which is one of the striking differences between the diode and YAG laser welding. In conduction mode welding, employed with the diode laser, the laser energy is absorbed at the surface of the workpiece and the weld pool is developed as heat is conducted through the material. The YAG laser provides for keyhole mode welding in which the laser beam penetrates the surface of the weld pool by vaporising some material. Narrow, deep penetration welds are possible with keyhole mode welding. The transition between conduction and keyhole modes depends on the energy density in continuous wave laser welding processes.[9]

Welding and sample preparation

Full penetration bead on plate welds were produced with Nd:YAG and diode lasers at the speeds of 6·0 and 1·6 m min^{-1} respectively. The weld was top shielded by Ar at a flow rate of 30 L min^{-1}. Welds were made perpendicular or parallel to the rolling direction. After welding, transverse samples were cut from representative welds for polishing, etching and metallographic observation. Cross-weld Vickers microhardness testing was conducted on nital etched samples under a load of 500 g with a loading time of 15 s.

Uniaxial tensile testing

Room temperature uniaxial tensile tests were also performed on parent metal specimens machined to ASTM-E8 standard size using a crosshead speed of 4 mm min^{-1}. Welded specimens were prepared with the weld oriented both longitudinal and transverse to the loading direction.

Formability testing

The formability of both welded and unwelded blanks was evaluated using the limiting dome height (LDH) test. The experimental set-up is shown in Fig. 3. The specimens were carefully placed to locate the weld line at the centre of the dome punch. A 101·6 mm diameter hemispherical punch was used at a velocity of 1 m min^{-1}. Draw-in of the blank was resisted by draw bead dies to assure a pure stretching condition. The resulting stress state was nearly biaxial, with strain in both transverse (perpendicular) and longitudinal (parallel) directions with respect to the weld line. Each coupon was stretched to failure and the limiting dome height was taken at the peak punch load. To minimise friction between the punch and sheet, specimens were degreased, deburred, and lightly coated with mineral oil. The dies were thoroughly cleaned before each test. The welded samples were positioned with the top of the weld facing out so that the punch made contact with the root side. Three samples were tested at each condition. The fracture surfaces after formability testing were then examined using SEM.

Table 2 Characteristics of two lasers

Laser type	Power, kW	Focal length, mm	Beam size,mm
Diode	4	80	$12 \times 0{\cdot}5$
Nd:YAG	3	200	0·6

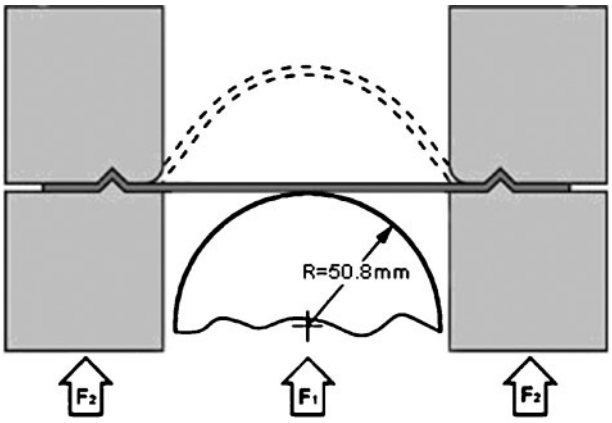

3 Tooling geometry of LDH test: specimen after deformation is shown by broken lines

Results

Cross-weld hardness profiles and related microstructure

Representative cross-weld hardness profiles for DP980 and HSLA welded with both laser types are shown in Fig. 4. The base metal hardness for DP980 was 294 HV, while the HSLA was 163 HV. The weld hardness characteristics for both steels under both lasers are summarised in Tables 3 and 4. For weldments made with both lasers and fusion zone hardness for both steels was significantly higher than that of the base metal and decreased gradually through the HAZ to the unaffected base metal. The average fusion zone hardness for the DP980 with YAG laser welding conditions was 430 HV and the corresponding fusion zone microstructure was fully martensitic, as shown in Fig. 5*a*. For YAG welds on the HSLA, the average fusion zone hardness was 302 HV. The inspection of its fusion zone microstructure, shown in Fig. 5*b*, revealed that it was predominantly martensitic. Since the weld heat input, and thus cooling rates, for these two specimens were similar, the difference in fusion zone hardness was attributed

Table 3 Weld hardness characteristics with YAG laser welding process

	Fusion zone		Softened zone	
	Hardness, HV	Width, mm	Hardness, HV	Width, mm
DP980	430	1·12	269	0·5
HSLA	302	1·07	No softening	

Table 4 Weld hardness characteristics with diode laser welding process

	Fusion zone		Softened zone	
	Hardness, HV	Width, mm	Hardness, HV	Width, mm
DP980	420	3·6	246	0·9
HSLA	222	3·1	No softening	

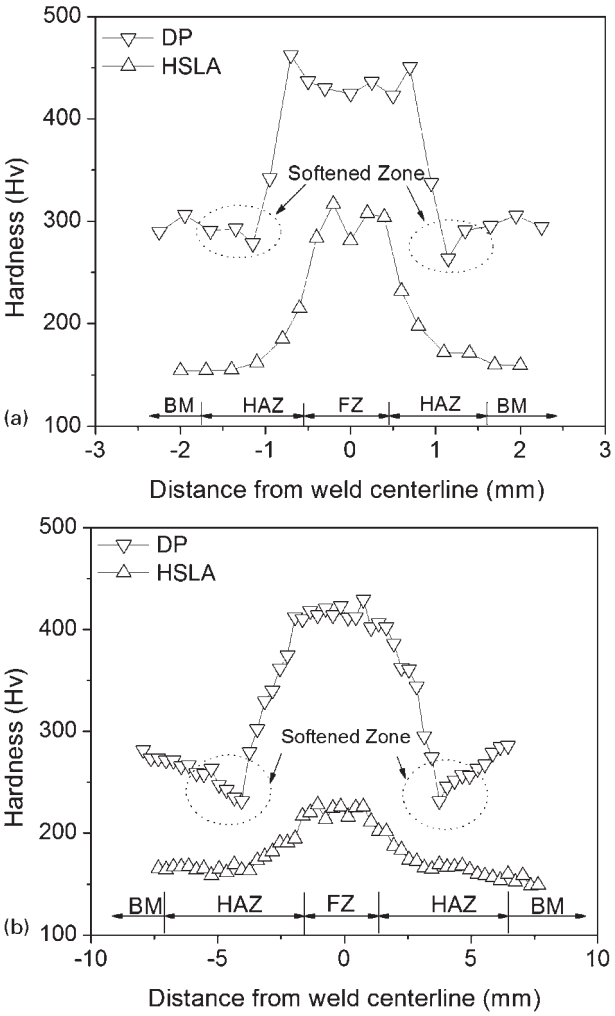

4 Cross-weld hardness profiles with *a* YAG laser at welding speed of 6·0m min^{-1} and *b* diode laser at welding speed of 1·6 m min^{-1}

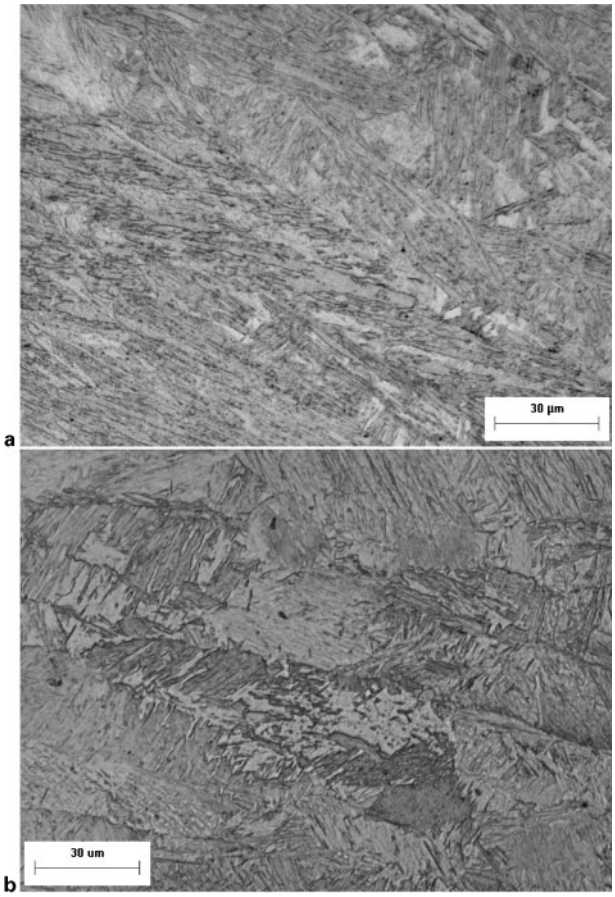

a DP980; *b* HSLA

5 Fusion zone microstructure with YAG laser welding

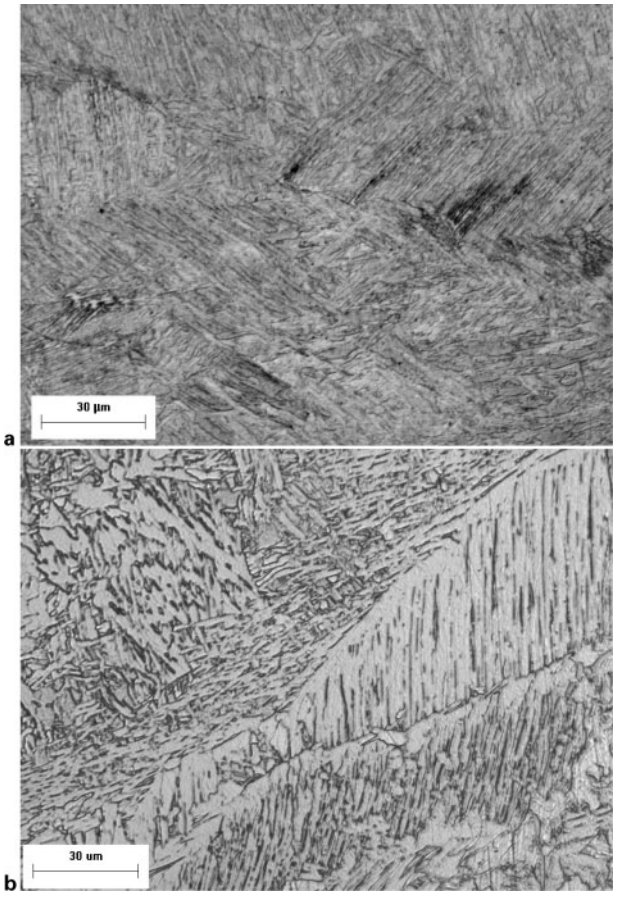

a DP980; *b* HSLA

6 Fusion zone microstructure with diode laser welding

predominantly to composition. From Table 1, the carbon content of DP980 was significantly higher than HSLA, at 0·135 and 0·056% respectively.

As for the diode laser welding process, the fusion zone hardnesses were less than those in corresponding YAG weldments. For DP980, fusion zone hardness was slightly lower than in the YAG laser welded fusion zone and its microstructure was similar (Fig. 6*a*). For HSLA, the diode welds' fusion zone hardness and microstructure showed great difference from the YAG weldments. The diode laser welded fusion zone microstructure was mainly ferritic, as shown in Fig. 6*b*.

A hardness 'valley' was observed in the outer HAZ of the DP980 weld, in which the local hardness dropped below the base metal hardness. This softened region has previously been observed in the HAZ of DP steels[3,4] and resulted from local tempering of the original martensite phase. In this region, the peak temperature during the welding cycle was below the Ac_1 temperature (the critical temperature for re-austenisation during heating process), and as a result, no austenitisation of the C rich martensite phase occurred. The high temperature exposure promoted martensite decomposition. The average minimum hardness in this valley was 269 HV for YAG laser welding process, 25 HV lower than the base metal, which indicates that the martensite has

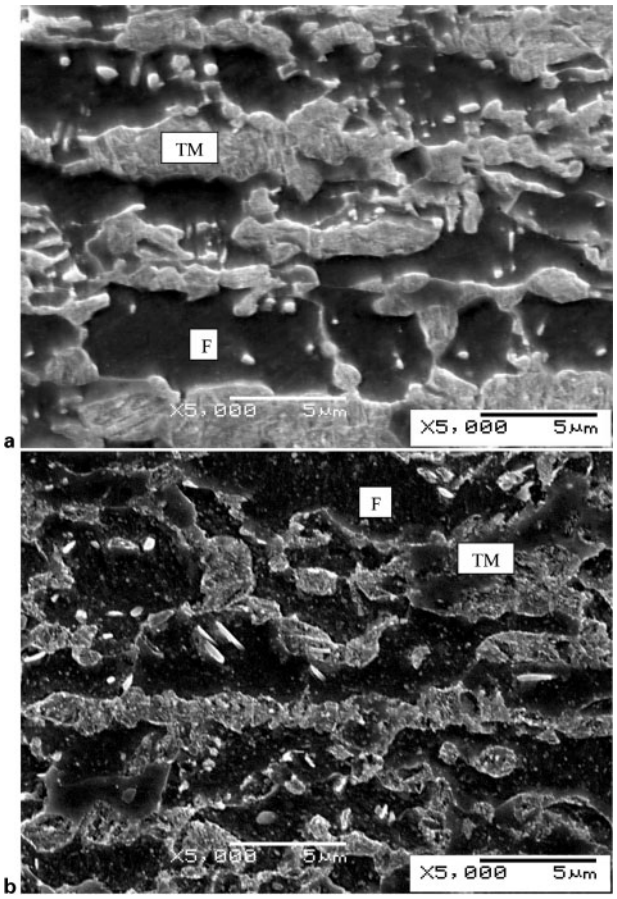

7 Softened zone microstructure with *a* YAG laser welding at speed of 6·0 m min^{-1} and *b* diode laser welding at speed of 1·6 m min^{-1}

partially decomposed in the softened zone, as shown in Fig. 7*a*. As for the HAZ softened zone with diode laser welding, martensite exhibited much more severe decomposition as shown in Fig. 7*b* and resultant lower minimum hardness value (246 HV). The difference was attributed to the different working mode of these two lasers as described above. When using the YAG laser in keyhole mode, higher welding speed could be achieved and as a result, the welds were made with much lower heat input than with the diode laser under the same power, thus resulting in shorter times at elevated temperatures and faster post-weld cooling.

The base metal microstructure of the HSLA contained no martensite, thus there was no observable softening in the cross-weld hardness profiles. Rather, there was a continuous transition from the fusion zone to the base metal in the hardness distribution profile.

Uniaxial tensile testing

Typical engineering stress–strain curves for the DP980 and HSLA parent metals are shown in Fig. 8. As expected, the DP980 showed continuous yielding to a high tensile stress without the yield point elongation observed in the HSLA. The HSLA had significantly lower tensile strength and greater elongation than the DP980. The HSLA did not show any effect of rolling direction orientation in the tensile results. The DP980, on the other hand, exhibited higher strength and lower elongation in the orientation parallel to the rolling direction compared to the perpendicular orientation. Thus, the DP980 exhibited anisotropic behaviour. The detailed tensile testing results for both base metals are shown in Table 5.

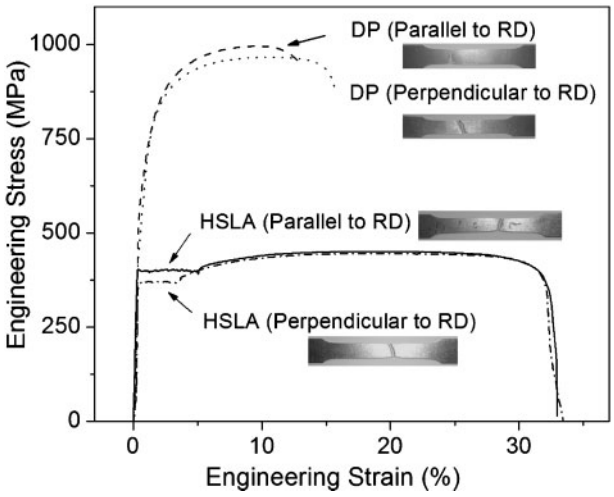

8 Typical stress–strain curves of parent metals

The tensile test results of the welded DP980 samples with the rolling direction parallel to the loading direction are summarised in Table 6. The total elongations of the DP980 weldments with weld transverse to the specimen axis were much lower than that of the parent metal. Visual observation of the fractured specimens showed that strain was localised in the HAZ, with final fracture occurring in the softened region, parallel to the weld. Diode laser welded specimens showed lower strength and total strain due to more severe softening than was present in YAG laser welds. The tensile strength of the DP980 weldments with welds parallel to and centred on the tensile specimen axis was higher than that of the base metal, since the tested samples were a composite of several different regions, including the hardened fusion zone, hardened and softened HAZ, and base metal. The longitudinal strain was slightly lower than the base metal. In this case, failure initiated in the fusion zone as a result of decreased ductility in the hardened weld metal.

Formability testing

Biaxial stretch formability testing for parent metal and welded blanks was performed by standard LDH testing. The top views of the parent metal LDH test specimens after fracture are shown in Fig. 9. Fracture in the HSLA parent metal followed a crescent shaped path around the

Table 5 Tensile properties of parent metal

	Parallel to RD		Perpendicular to RD	
	Strength, MPa	Strain, %	Strength, MPa	Strain, %
DP980	997±20	9·8±0·3	963±9	10·5±0·3
HSLA	451±0	19·5±1	444±0·6	21·4±0·9

Table 6 Tensile properties of DP980 weld

	Longitudinal		Transverse	
	Strength, MPa	Strain, %	Strength, MPa	Strain, %
YAG	1051±28	7·9±0·9	965±5	5·4±0·1
Diode	1173±15	3·3±0·1	775±13	2·9±0·1

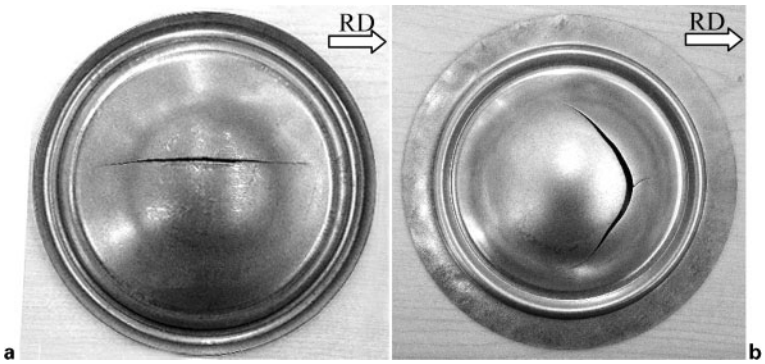

a DP980; *b* HSLA

9 Top views of LDH specimens for parent metals

centre of the dome. Fracture in the DP980 parent metal differed as it followed a straight path located a short distance (17 mm) from the centre of the dome. The orientation of the fracture path was parallel to the rolling direction. Ductility in the perpendicular direction was exhausted first causing fracture initiation and propagation along the longitudinal direction.

Figure 10 shows top views of YAG laser welded blanks. No influence of the rolling direction on the failure mode was found for either steel, which was also true for diode laser welded coupons, shown in Fig. 11. The fracture location and path in the HSLA welded blanks was similar to the parent metal. Fracture apparently initiated at the weld where ductility was exhausted and propagated perpendicular to the weld line, following a crescent shaped path. The distance from the fracture sites to the dome apex was nearly the same between the HSLA welded blanks and parent metal, $\sim$30 mm. Fracture in the DP welded blanks was located within the HAZ in a direction parallel to the weld. The fracture sites corresponded to the softened zone, as confirmed by the weld hardness distribution.

In terms of dome height, shown in Fig. 12, the LDH values for the parent metal HSLA and DP980 were 32·9 and 30·3 mm respectively. No definite relationship was observed between the LDH and weld orientation relative to rolling direction, as the LDH values were within the same range for the perpendicular and parallel weld directions respectively. There was negligible reduction in formability caused by welding on the HSLA steel, as shown in Fig. 12*a*. In contrast, the LDH of the welded DP980 blanks was significantly lower than that of the parent metal (Fig. 12*b*), decreasing $\sim$50%. Furthermore, there was no observed relationship between weld orientation with respect to rolling direction and LDH. In both cases, failure was localised in the softened zone and propagated within this region. However, diode laser welded blanks had a slightly lower LDH than the corresponding YAG laser welded blanks.

Discussion

Many factors such as mechanical and metallurgical properties, die and punch geometry, lubrication, sheet

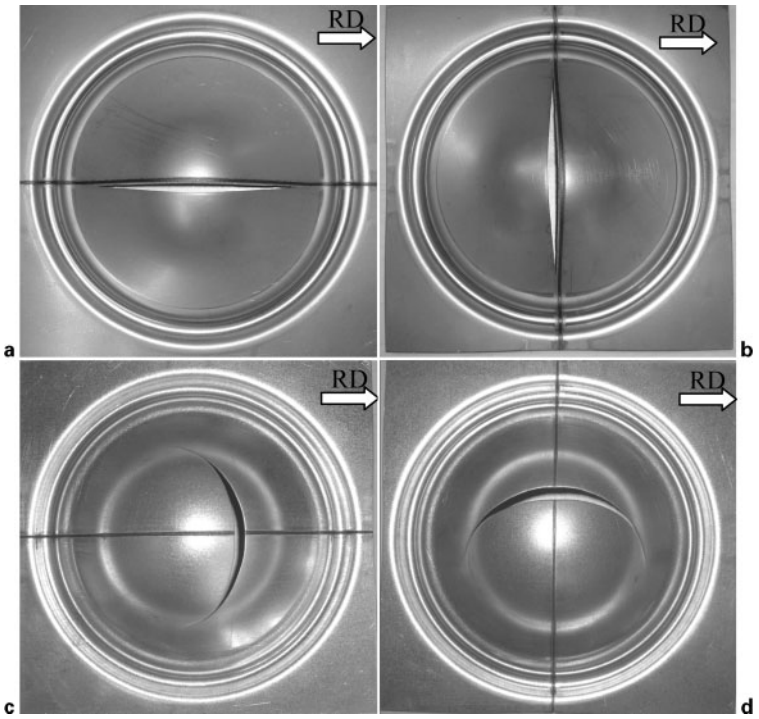

a DP980 with weld parallel to RD; *b* DP980 with weld perpendicular to RD; *c* HSLA with weld parallel to RD; *d* HSLA with weld perpendicular to RD

10 Top view of LDH of YAG laser welded specimens

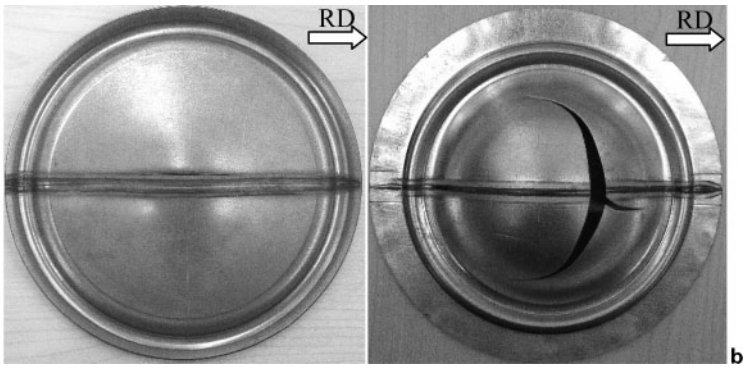

a DP980; *b* HSLA

11 Top view of LDH of diode laser welded specimens

thickness, sheet roughness, punch speed, etc. affect formability to varying degrees and with interdependent relationships.[10] In this work, extraneous conditions were kept as constant as possible. The formability testing results were characterised in two ways: by failure mode (i.e. crack initiation and propagation) and by the dome height at failure

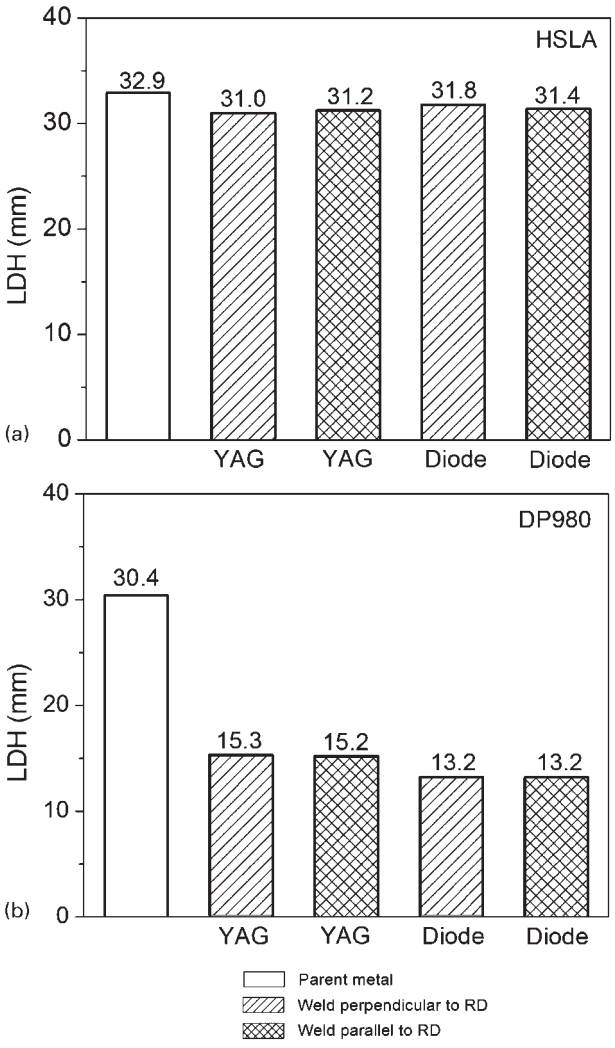

a DP980; *b* HSLA

12 Limiting dome height of parent metals and welded blanks

Parent metal

Results showed that the DP980 parent metal had a dome height approaching that of HSLA. Compared to previous formability research conducted on DP steels,[11] the volume fraction of martensite in DP980 of the present study was much higher and the martensite displayed a banded morphology. The banded martensite resulted in slightly anisotropic behaviour in uniaxial tensile testing. Anisotropic behaviour of the DP980 base metal was also seen in biaxial testing, as discussed below.

First, the effect of the DP980 anisotropy was manifested in the failure mode difference as compared to the HSLA on a macroscale level. For the HSLA, the peak strain or failure site was 30 mm from the dome apex and no remarkable influence on the failure mode was exerted by the rolling direction or texture. For DP980 base metal, the failure site was 17 mm from the specimen centre and always propagated along the rolling direction. Different peak strain location between the two parent metals is believed to be caused by combined factors like microstructural difference, different surface conditions and sheet thickness.[12,13]

On a microscale level, as martensite and ferrite, the two phases in DP steel, have markedly different mechanical properties, the composite nature of this material was found to be a significant factor. Ferrite can be considered a ductile phase with low strength, whereas martensite is relatively less ductile and considerably stronger. The two phases are not necessarily plastically homogeneous, and the ferrite phase may show earlier and greater deformation than the martensite phase. In fact, it was not readily evident in this study whether the martensite phase deformed plastically, or was limited to the elastic regime. Nevertheless, failure occurred when inhomogeneous deformation eventually promoted microvoid formation. The interface between martensite/ferrite was found to facilitate the formation of cracks or voids due to decohesion at the phase boundary. This is illustrated in Fig. 13*a*, which shows void formation along the martensite/ferrite interfaces near the final failure location under biaxial testing. The microcracks extended by the linking of growing voids and the ferrite/martensite interfaces provided a preferential crack path. The SEM fractograph in Fig. 13*b* shows the presence of smooth surfaces interspersed with well developed dimpled areas. Most of the smooth areas were thought to be former ferrite/martensite interfaces, while the dimpled areas were locations of ductile rupture

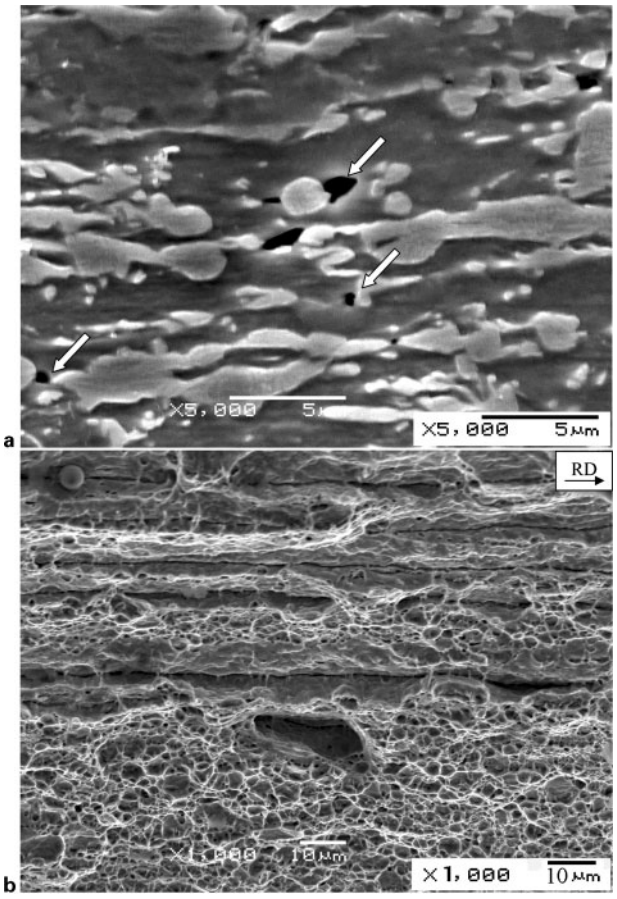

13 Observation using SEM on DP980 parent metal of *a* cross-section and *b* fracture surface morphology

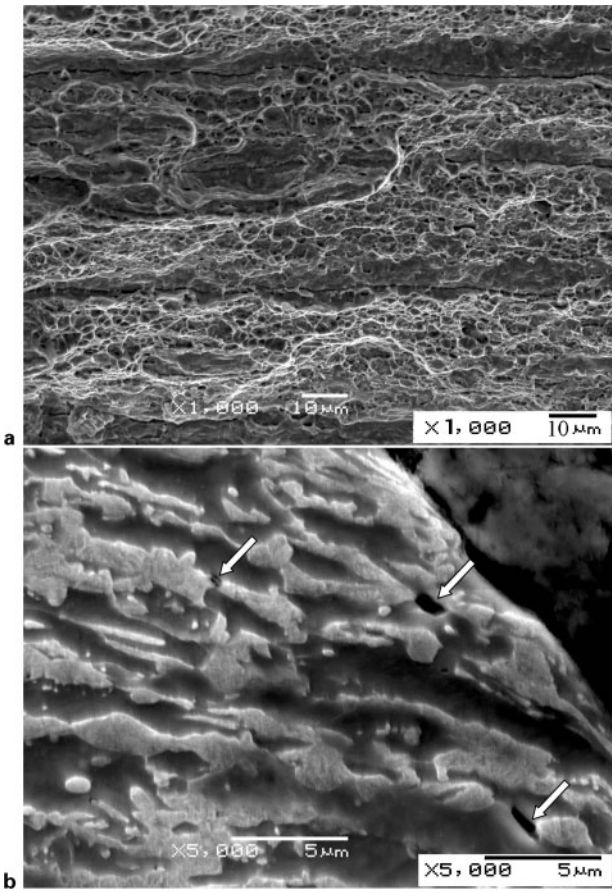

14 Observation using SEM on YAG laser welded DP980 blanks of *a* fracture surface morphology and *b* cross-section

of the ferrite matrix, the more continuous phase in the parent metal. The banded martensite 'stringers' provided a longer mean free path along the ferrite/martensite interfaces and hence, an easier crack propagation path along the rolling direction. Thus, in LDH formability testing of the DP980, the crack followed a straight line along the rolling direction.

Welded blanks

For the HSLA welded blanks, there was only a slight decrease in dome height from the parent metal, as shown in Fig. 12*a*. It was observed during stretch forming that fracture initiated at the fusion zone and propagated perpendicularly to the weld line, through the HAZ, and into the unaffected base metal. In LDH testing, principal strain in the welded specimens can be divided into two components with respect to the weld line: longitudinal and transverse. The hardness of the fusion zone and HAZ was higher than the base metal and the ductility was lower. Formability was then limited in the longitudinal direction and failure always initiated in the fusion zone. The welded blanks still exhibited high dome height, probably due to the narrow fusion zone and its rather ductile microstructure, namely bainite and low carbon martensite. The same failure mode has also been observed by other researchers in CO_2 laser welds on DP steels, in which failure occurred in the fusion zone due to severe hardening but with no softened zone being reported.[14]

The failure mode in DP980 welded blanks was completely different from that of the HSLA welded blanks as fracture was located in the softened zone and not in the fusion zone. The softened zone formation apparently dominated the influence of base metal anisotropy regardless of the orientation between weld and rolling direction. The LDH testing induced both longitudinal and transverse stretching. The transverse strain resulted in localised deformation in the softened zone due to its lower strength compared to the hardened fusion zone/HAZ and adjacent base metal. Fracture occurred as ductility in the softened zone was exhausted.

Two cases of fracture morphology, taking the YAG weld as an example, can be considered depending on the orientation of the weld with respect to the rolling direction. In the first case, when the weld line was oriented parallel to the rolling direction, the direction of failure was similar to the parent metal. The fracture surface, shown in Fig. 14*a*, had a similar morphology to that observed in Fig. 13*a*. Regions of ductile rupture were interspersed with blocky regions that were aligned with the rolling direction. These blocky areas were regions of tempered martensite. The tempered martensite islands consisting of iron carbide aggregates were still plastically inhomogeneous with the ferrite matrix, and as a result, served as void initiation sites during plastic strain, which was shown in Fig. 14*b*. The second case, where the weld was oriented perpendicular to the rolling direction, could be expected to demonstrate improved formability characteristics since the preferential crack propagation direction of the parent material was orthogonal to the weld line and corresponding

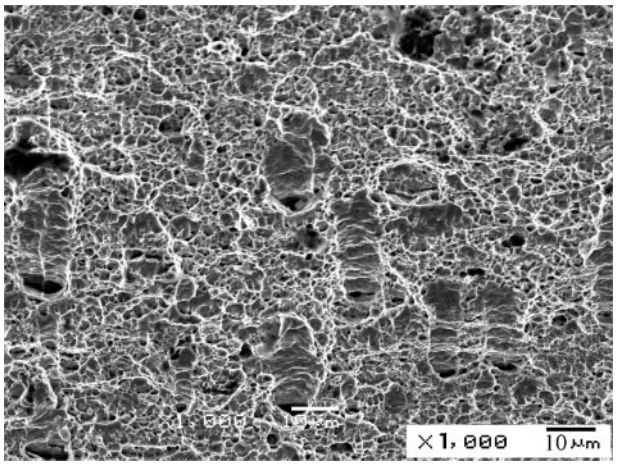

15 Fracture surface of YAG laser welded DP980 blanks after LDH testing with weld perpendicular to RD

softened zone where transverse strain was localised. Experimental results showed that this was not the case, as the LDH was similar regardless of weld orientation. Even though the orientation had changed, the softened zone dimension and tensile properties were constant. The fracture surface in Fig. 15 shows a dissimilar appearance to the fracture surface in the preceding case. The ferrite matrix showed ductile rupture and areas of tempered martensite can still be observed, but in this case fracture propagated both through the prior martensite regions and around them.

Softened zone and LDH

Gleeble thermal simulation was used to reproduce the softened zone microstructure across a uniform tensile test specimen. The thermal history governed by four parameters shown in Fig. 16 was tailored to match typical laser welding cooling rates under similar conditions to the experimental parameters. Tensile tests on Gleeble specimens with a peak temperature of 650°C showed increased elongation (21%) and lower strength (642 MPa) relative to the as received base metal (elongation: 9·8%; strength: 997 MPa). This confirms that even though the ductility of the softened region was improved over that of the base metal and harder fusion zone/HAZ, the low strength resulted in a strain

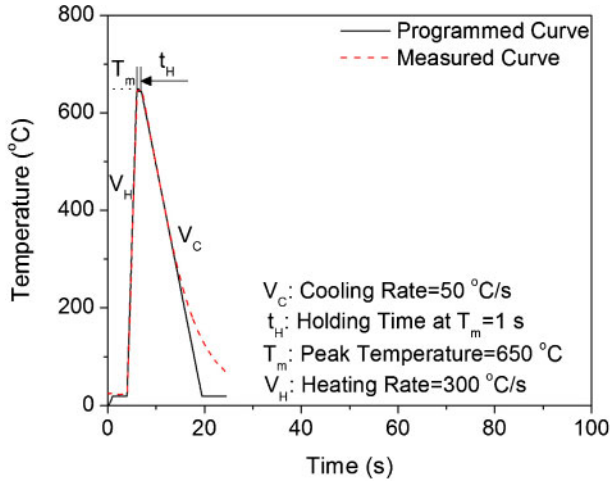

16 Thermal curves and related parameters in Gleeble simulations

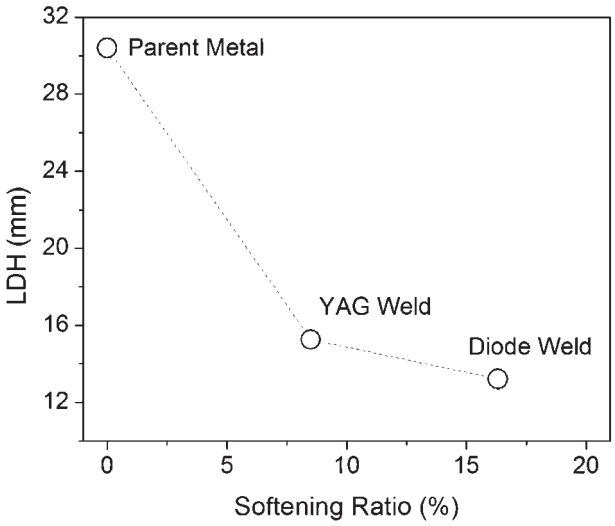

17 Relationship between softening ratio and LDH of DP980 parent metal and welded blanks

concentration and premature failure during LDH testing.

From the above, it could be found that welding process characteristics did exert a major influence on dome height. YAG laser welded blanks had a slightly greater height than those welded with diode laser regardless of their fusion zone hardness within the same range. It can be concluded that in the DP980 steel, the softened zone formation governed the formability behaviour as well as the failure mode described above. In order to compare formability of different weldments, a softening ratio R designed to reflect the inhomogeneity of mechanical properties across the weld was introduced as follows

$$R=\frac{Hv_{\mathrm{BM}}-Hv_{\mathrm{SZ}}}{Hv_{\mathrm{BM}}}\times 100\%$$

Hv_{SZ} and Hv_{BM} refer to the softened zone and base metal hardness respectively.

The relationship between R and LDH is shown in Fig. 17. With increasing the mechanical inhomogeneity, namely R, the LDH showed a decrease. The result could be explained as follows. In the parent metal (R=0), the deformation or strain was well distributed over a wider region, compared to the welded blanks ($0<R<1$) where the deformation was increasingly concentrated along a narrow softened region. In diode laser welded blanks, the softened zone showed a greater hardness decrease and a bigger strength difference between the unaffected base metal. As a result, in the deformation process, the deformation was more severely concentrated in the softened zone due to lower contribution from the uniform deformation of the unaffected base metal. So the softened zone caused a much earlier failure in the formability testing process, i.e. lower LDH.

Conclusions

Two steels, namely DP980 and HSLA, were chosen to evaluate the influence of base metal tensile properties and laser welding process on formability behaviour from the standpoint of failure mode and limiting dome height. The investigated steels both had a ferrite matrix and secondary strengthening phase (martensite and carbide

respectively). DP980 showed slightly anisotropic behaviour mainly arising from dispersed banded martensite whereas HSLA was isotropic. Fracture pattern development under the biaxial LDH forming process was investigated on a microscale level on DP parent metal and welded blanks respectively. The conclusions can be drawn as follows.

1. In LDH formability testing on parent metals, different failure path was exhibited between two steels even with similar dome height. Dual phase was strongly sensitive to rolling direction in terms of failure mode whereas HSLA showed a more symmetrical failure pattern and path due to its isotropic behaviour.

2. In LDH formability testing on welded blanks, the HAZ softened zone in DP980 weldments completely dominated the fracture pattern: it was the vulnerable region in which the failure always initiated. Rolling direction did not show any influence on formability or fracture pattern of welded blanks. However, the failure path of HSLA welded blanks was initiated at the weld and propagated into the unaffected base metal. Two steels showed totally different response to the laser welding process in terms of formability behaviour.

3. It was found that void initiation at large local strains occurred by decohesion at the interfaces of matrix and secondary phase (martensite and tempered martensite) due to their different mechanical performance in both DP980 parent metal and welded blanks. And furthermore, fracture propagated preferentially along these interfaces. The difference between the parent metal and welded blanks was that in the latter, void initiation was limited to a very narrow band of softened zone.

4. The softened zone in the welded blanks had a higher ductility but lower strength than the DP980 base metal. The local ductility improvement in the softened zone did not benefit the welded blanks' formability. YAG laser welded blanks had a higher LDH than diode laser weldments probably due to a greater contribution from the uniform deformation of the unaffected base metal.

Acknowledgements

The authors would like to thank Prof. Norman Richards and Jonathon Drabik from the University of Manitoba for the Gleeble thermal simulation work. This work was financially supported by Auto21 (www.auto21.ca), Dofasco, Huys Industries Ltd, Centerline Ltd, and the International Lead Zinc Research Organization (USA).

References

1. W. Bleck: *J. Met*., 1996, **48**, 26–30.
2. M. Sarwar and R. Priestner: *J. Mater. Sci*., 1996, **31**, 2091–2095.
3. M. Xia, N. Sreenivasan, S. Lawson, Y. Zhou and Z. Tian: *J. Eng. Mater. Technol*., 2007, **129**, 446–452.
4. P. K. Ghosh, P. C. Gupta, R. Avtar and B. K. Jha: *ISIJ Int*., 1990, **30**, 233–240.
5. C. Hsu, P. Soltis, M. Carroscia, D. Barton and C. Occhialini: Proc. Sheet Metal Welding Conf. XI, American Welding Society (Detroit Section) Sterling Heights, MI, USA, May 2004, 1–11.
6. E. Biro and A. Lee, 2004: Proc. Sheet Metal Welding Conf. XI, American Welding Society (Detroit Section) Sterling Heights, MI, USA, May 2004, 1–11.
7. W. Gan, S. S. Babu, N. Kapustka and R. H. Wagoner: *Metall. Mater. Trans. A*, 2006, **37A**, 3221–3231.
8. M. I. Khan, M. L. Kuntz, P. Su, A. Gerlich, T. H. North and Y. Zhou: *Sci. Technol. Weld. Join*., 2007, **12**, (2), 175–182.
9. M. P. Miles, J. Pew, T. W. Nelson and M. Li: *Sci. Technol. Weld. Join*., 2006, **11**, (4), 384–388.
10. C. Ma, S. D. Bhole, D. L. Chen, A. Lee, E. Biro and G. Boudreau: *Sci. Technol. Weld. Join*., 2006, **11**, (4), 480–487.
11. H. Shao, J. Gould and C. Albright: *Metall. Mater. Trans. B*, 2007, **38B**, 321–331.
12. W. W. Duley: 'Laser welding'; 1999, New York, John Wiley & Sons, Inc.,
13. J. R. Fekete: *Soc. Autom. Eng*., 1997, **106**, 699–710.
14. M. Y. Demeri: *Metall. Trans. A*, 1981, **12A**, 1187–1196.